



## A High-Performance Rechargeable Iron Electrode for Large-Scale Battery-Based Energy Storage

Aswin K. Manohar,\* Souradip Malkhandi,\*\* Bo Yang,\* Chenguang Yang, G. K. Surya Prakash,\*\* and S. R. Narayanan\*\*<sup>z</sup>

Loker Hydrocarbon Research Institute, Department of Chemistry, University of Southern California, Los Angeles, California 90089, USA

Inexpensive, robust and efficient large-scale electrical energy storage systems are vital to the utilization of electricity generated from solar and wind resources. In this regard, the low cost, robustness, and eco-friendliness of aqueous iron-based rechargeable batteries are particularly attractive and compelling. However, wasteful evolution of hydrogen during charging and the inability to discharge at high rates have limited the deployment of iron-based aqueous batteries. We report here new chemical formulations of the rechargeable iron battery electrode to achieve a ten-fold reduction in the hydrogen evolution rate, an unprecedented charging efficiency of 96%, a high specific capacity of 0.3 Ah/g, and a twenty-fold increase in discharge rate capability. We show that modifying high-purity carbonyl iron by in situ electro-deposition of bismuth leads to substantial inhibition of the kinetics of the hydrogen evolution reaction. The in situ formation of conductive iron sulfides mitigates the passivation by iron hydroxide thereby allowing high discharge rates and high specific capacity to be simultaneously achieved. These major performance improvements are crucial to advancing the prospect of a sustainable large-scale energy storage solution based on aqueous iron-based rechargeable batteries.  
© 2012 The Electrochemical Society. [DOI: 10.1149/2.034208jes] All rights reserved.

Manuscript submitted April 17, 2012; revised manuscript received May 11, 2011. Published July 20, 2012.

Large-scale electrical energy storage systems are needed to accommodate the intrinsic variability of energy supply from solar and wind resources.<sup>1,2</sup> Such energy storage systems will store the excess energy during periods of electricity production, and release the energy during periods of electricity demand. Viable energy storage systems will have to meet the following requirements: (i) low installed-cost of <\$100/kWh, (ii) long operating life of over 5000 cycles, (iii) high round-trip energy efficiency of over 80%, and (iv) ease of scalability to megawatt-hour level systems.<sup>2</sup> Rechargeable batteries are particularly suitable for such large-scale storage of electrical energy because of their high round-trip efficiency and scalability. Among the types of rechargeable batteries under consideration are vanadium-redox, sodium-sulfur, zinc-bromine, zinc-air and lithium-ion batteries.<sup>3,4</sup> In addressing the challenges of durability, cost, and large-scale implementation of the foregoing types of batteries, the beneficial features of iron-based alkaline batteries for large-scale energy storage have been largely overlooked. Nickel-Iron batteries have been used in various stationary and mobile applications for over 70 years in the USA and Europe until the 1980s when the iron-based batteries were largely supplanted by sealed lead-acid batteries. Iron-air batteries because of their high specific energy underwent active development for electric vehicles and military applications in the 1970s after the “oil shock” but major research in this area was abruptly discontinued after 1984. Except for some seminal research in India by Shukla et al. during the period 1986–1992, iron electrodes have not received any significant attention.<sup>5–7</sup> We emphasize in a recent article that despite being less conspicuous in common applications, iron-based alkaline batteries such as “iron-air” and “nickel-iron” batteries have unique characteristics that make them very attractive and highly suitable for meeting the emerging need of grid-scale electrical energy storage systems.<sup>8,9</sup>

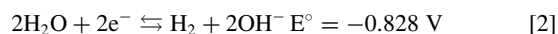
The electrochemistry of the iron electrode in alkaline batteries involves the redox process involving iron (II) hydroxide and elemental iron:



The forward reaction occurs during charging of the electrode and the reverse reaction occurs during discharge.

Iron, the primary raw material for iron-based battery systems, is globally abundant, relatively inexpensive, easily-recycled, and eco-friendly. Also, the iron electrode is well-known for being robust over repeated cycles of charge and discharge. Stable performance over

3000 charge and discharge cycles has been reported in nickel-iron batteries.<sup>10–13</sup> Such robustness is extraordinary as most rechargeable battery electrodes degrade within 1000 cycles. The robustness of the iron electrode is attributed to the low solubility of the hydroxides of iron in alkaline media. The principal limitation of the iron electrode is its low charging-efficiency that is in the range of 55–70%.<sup>13–16</sup> This limitation arises from the wasteful hydrogen evolution that occurs during charging according to the following reaction.



The hydrogen evolution reaction occurs because the electrode potential for this reaction is positive to that of the iron electrode reaction (Equation 1). Consequently, batteries will have to be overcharged by 60–100% to achieve full capacity. The hydrogen evolution that occurs during charging is undesirable because it lowers the round-trip energy efficiency and results in loss of water from the electrolyte. Thus, suppressing hydrogen evolution at the iron electrode has far-reaching benefits of raising the overall energy efficiency, lowering the cost, and increasing the ease of implementation of iron-based batteries in large-scale energy storage systems. However, suppressing hydrogen evolution and achieving an iron electrode with a charging-efficiency close to 100%, without interfering with the other performance features of the electrode, has been a formidable challenge for many years.

Another limitation of commercially available iron batteries is their inability to be discharged at high rates; when discharged in less than five hours (also termed the five-hour rate) the capacity realized is very small. Grid-scale electrical energy storage requires that the battery be capable of being charged and discharged in one to two hours. The discharge rate capability of the iron electrode can be improved if the passivation by the electrically non-conductive iron (II) hydroxide, (the discharge product) can be mitigated (Equation 1). Shukla et al. have demonstrated the beneficial role of various additives on mitigating passivation.<sup>17,18</sup> However, achieving high rate capability and high efficiency simultaneously continues to be a challenge.

For the first time, we demonstrate a stable high-performance iron electrode in which we achieve a ten-fold decrease in hydrogen evolution rate without interfering with the kinetics of the iron electrode reaction. With this level of suppression of hydrogen evolution, the charging efficiency has reached an unprecedented value of 96%. We also report a specific charge storage capacity of 0.3 Ampere-hour g<sup>-1</sup> and this is among the highest values reported for iron electrodes without any overcharge.<sup>19</sup> Furthermore, this new iron electrode can also be charged and discharged rapidly, meeting yet another important requirement for large-scale energy storage. This new generation of high-performance electrodes overcomes the long-standing drawbacks and finally enables iron-air and nickel-iron technologies to become

\*Electrochemical Society Student Member.

\*\*Electrochemical Society Active Member.

<sup>z</sup>E-mail: sri.narayan@usc.edu

the basis of inexpensive, efficient and robust energy storage systems for grid-scale applications. We are applying this type of iron electrode in our efforts to realize an “iron-air” battery capable of 5000 cycles with a round-trip energy efficiency of 80% and costing less than US \$100 per kilo Watt-hour.

The advanced iron electrode reported here results from a unique combination of iron materials and additives selected based on their ability to inhibit the hydrogen evolution reaction and enhance discharge rate capability. The rechargeable iron electrodes in commercial nickel-iron batteries are prepared from purified magnetite ore ( $\text{Fe}_3\text{O}_4$ ) or by the chemical reduction of ferric oxide or other precursors.<sup>5,13,17</sup> In our research, the electrodes were prepared from high-purity “carbonyl iron powder.” “Carbonyl iron powder” consists of spherical iron particles (3–5 micron diameter) produced by the decomposition of iron pentacarbonyl. This material was post-treated in hydrogen at 300°C to remove any residual oxygen and carbon. Upon such heat-treatment the unique “onion” structure of carbonyl iron is erased and the microstructure becomes homogeneous. Carbonyl iron powder, consisting of  $\alpha$ -iron, is one of the purest forms of iron available commercially. We have confirmed here that using such high-purity iron material is an important aspect of electrode formulation for inhibiting the hydrogen evolution reaction and achieving high charging efficiency. To further improve the charging efficiency and achieve near complete suppression of hydrogen evolution, we recognized the need to incorporate minute amounts of other materials that can remain on the surface of carbonyl iron and inhibit the kinetics of hydrogen evolution. Therefore, in these carbonyl iron electrodes, we also incorporate elemental bismuth by in situ electro-reduction of bismuth sulfide that effectively suppresses hydrogen evolution and also improves the discharge rate and utilization of the active materials. Bismuth is ideally suited for this application because it is non-toxic and does not compromise the eco-friendliness of the iron materials.

The manufacturing cost consideration is very important for meeting the challenging cost goals for large-scale energy storage as envisioned by the U. S. Department of Energy -ARPA-E. Consequently, we have focused on a low-cost approach to preparing electrodes. We have prepared “pressed-plate” type electrodes by combining the iron active material with a polyethylene binder material followed by the application of heat (Figure 1). Such electrodes are inexpensive to fabricate. Alternate methods of electrode fabrication such as sintering, which use high temperature treatment in an inert gas atmosphere, entail much higher costs and are therefore less attractive compared to the “pressed-plate” type electrodes reported here.<sup>20,21</sup>

### Experimental

The electrodes typically consisted of 81 w/w% carbonyl iron (SM grade BASF), 10 w/w% potassium carbonate and 9 w/w% polyethylene binder (MIPELON, Mitsui Chem USA). In yet another formulation, 5% of the carbonyl iron was substituted with bismuth sulfide (Aldrich). The powder mixture was spread on a degreased nickel grid and pressed at a temperature of 140°C and a pressure of 5 kg  $\text{cm}^{-2}$ . The amount of iron in these electrodes corresponded to a calculated (theoretical) capacity of about 2 Ampere-hours. Commercial iron electrodes were obtained from nickel-iron batteries manufactured by Sichuan Changong Battery Co., and these electrodes consisted of magnetite and graphite, largely. The exact composition of these electrodes is not available.

The iron electrodes were tested in a three - electrode cell. A nickel oxide battery electrode of the sintered type was used as the counter electrode (Figure 2). A solution of potassium hydroxide (30 w/v%), similar to that used in iron-based rechargeable batteries, was used as the electrolyte. All potentials were measured against a mercury/mercuric oxide (MMO) reference electrode ( $E_{\text{MMO}}^{\circ} = +0.098$  V vs. the normal hydrogen electrode).

The charging efficiency, discharge rate capability, and the response to repeated charge/discharge cycling were measured with a 16-channel battery cycling system (MACCOR- 4200). The steady-state polariza-

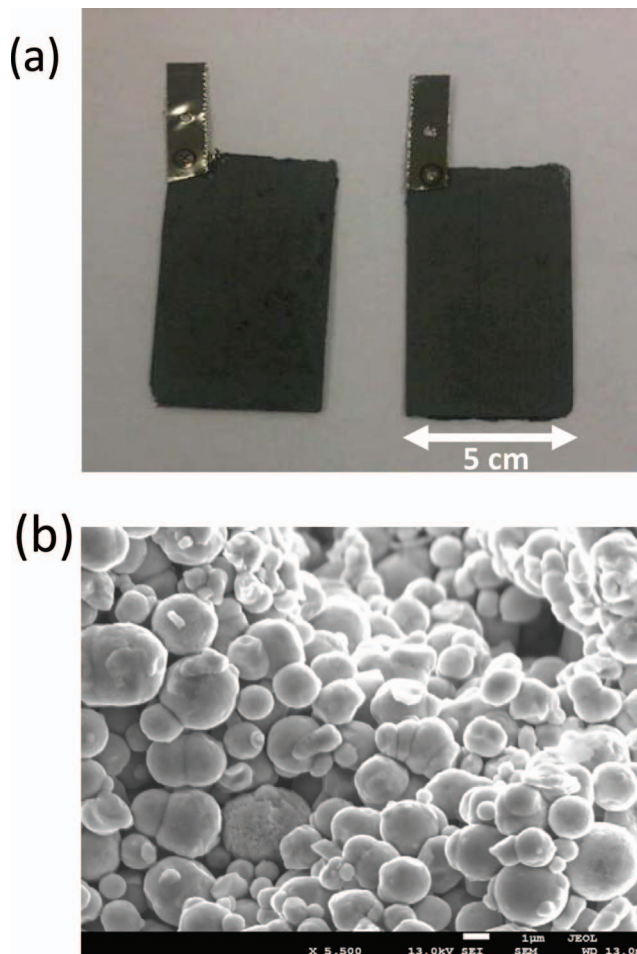


**Figure 1.** Electrode design (a) pressed-plate electrodes constructed from carbonyl iron powder (b) morphology of carbonyl iron powder in the electrode.

tion studies were conducted with a potentiostat/galvanostat (VMC-4, PAR Ametek).

The charging-efficiency was calculated as per the following:

$$\text{Charging Efficiency (\%)} = \{(Q_{\text{charging}} - Q_{\text{H}_2})/Q_{\text{charging}}\} \times 100 \quad [3]$$

where  $Q_{\text{charging}}$  is the total charge and  $Q_{\text{H}_2}$  is the charge used up in hydrogen evolution.

The hydrogen evolution current,  $I_{\text{H}_2}$  at the charging potential  $E$  was calculated using the Tafel relationship,

$$\text{Log}_{10}(I_{\text{H}_2}/I_0) = (E - E_{\text{H}}^{\circ})/b \quad [4]$$

where  $I_0$ , and  $b$ , are the exchange current and Tafel slope, respectively, determined from steady-state galvanostatic polarization

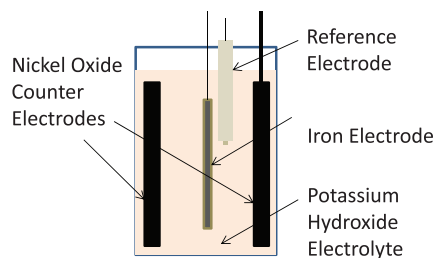


**Figure 2.** Test cell configuration showing iron working electrode, reference electrode and nickel oxide counter electrodes-2 Ah, electrolyte was 30% potassium hydroxide.

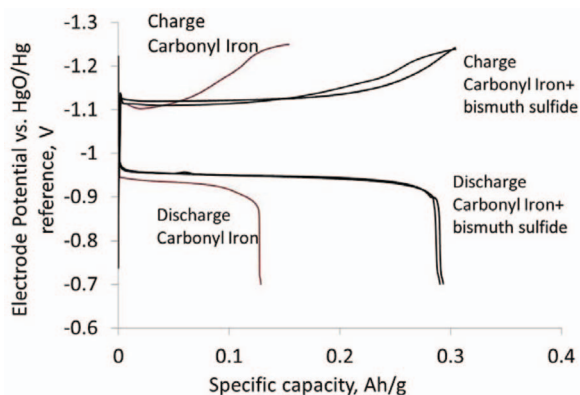


**Figure 3.** Typical charge and discharge voltage profiles for carbonyl iron electrodes with and without bismuth sulfide additive. Charge rate:  $C/2$  amperes (0.18 A for Carbonyl iron, 0.32 A for carbonyl iron + bismuth sulfide) discharge rate:  $C/20$  (0.018 A for carbonyl iron and 0.032 amperes for carbonyl iron + bismuth sulfide) and temperature, 20–25°C.

measurements.  $E_H^\circ$  is the standard potential for the hydrogen evolution reaction.

Specific capacity values for the carbonyl iron electrodes were calculated based on the carbonyl iron content, while for the commercial electrodes they were calculated based on the total mass of the material contained in the electrodes.

### Results and Discussion

**Charging-efficiency.**— The primary electrochemical process occurring during the charging of an iron electrode is the reduction of iron (II) hydroxide to iron (Eq. 1). However, hydrogen evolution (Eq. 2) also occurs simultaneously with the charging process. The diversion of part of the charging current toward the production of hydrogen results in low charging efficiencies.

Prior to measuring the charging efficiency, the pressed iron electrodes were charged and discharged about 30–40 times during which the discharge capacity increased to a stable value. The process of attaining a stable discharge capacity, termed “formation,” has been recognized previously for iron electrodes.<sup>5,17</sup> We have found that at the end of formation, the electrodes show a lower hydrogen evolution rate compared to the beginning of formation, a result that has not been reported for commercial electrodes. The formation process involves the repeated conversion of iron to iron (II) hydroxide followed by re-deposition as iron. This process could be expected to purify the carbonyl iron electrode further by the removal of any soluble impurities. All charging efficiency measurements were thus performed on such “formed” electrodes. The iron electrodes were charged to their rated capacity at  $C/2$  rate and discharged to a cut off voltage of  $-0.7V$  vs. MMO at  $C/20$  rate ( $C$  is the rated capacity of the electrode in Ampere-hours after formation, and  $C/n$  is the discharge current in Amperes). The voltage profiles during charge and discharge (Figure 3) show that the charge input is almost completely recovered during discharge.

Specifically, the charging efficiency (Eq. 3) of the carbonyl iron electrode was found to be  $90 \pm 1\%$ . The electrodes formulated with carbonyl iron and bismuth sulfide showed an even higher charge efficiency of  $96 \pm 1\%$  (Figure 4a). This high value of charge efficiency for the carbonyl iron electrode with bismuth sulfide represents a *ten-fold decrease* in the amount of hydrogen evolved during charging (Figure 4b).<sup>6,7,13–15,22</sup> Repeated cycling of these electrodes did not show any decline of this high value of charging efficiency (Figure 5).

The increase in charging efficiency found with the high-purity carbonyl iron electrode is attributed to the high overpotential for hydrogen evolution on carbonyl iron. Of the various iron electrode materials that were tested, the ones made from carbonyl iron have the highest overpotential for hydrogen evolution reaction (Figure 6).

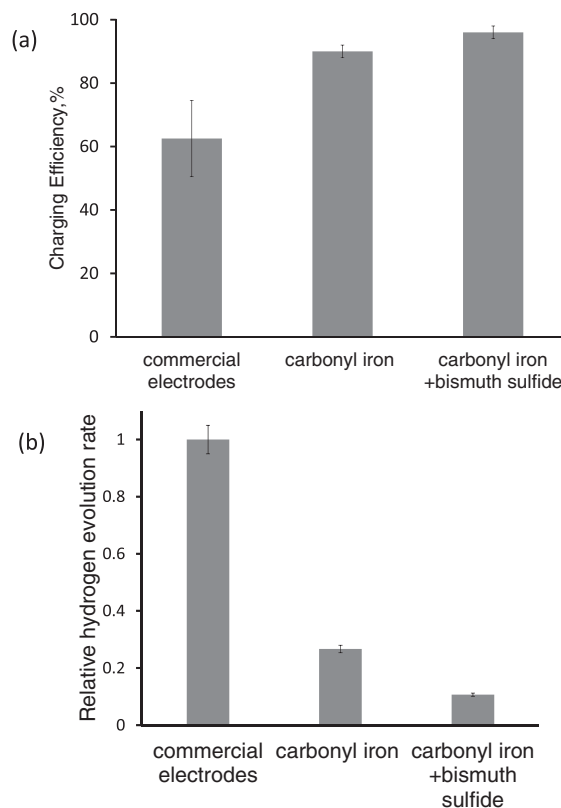


**Figure 4.** Electrochemical performance characteristics of iron electrodes: (a) charging efficiency at  $C/2$  rate for three types of electrode compositions, (b) relative rates of hydrogen evolution of various electrodes when charged at  $C/2$  rate.

Carbonyl iron does not contain the common impurities such as manganese, sulfur and phosphorus that are present in the reduced oxides. In general, these impurities decrease the hydrogen overpotential and facilitate hydrogen evolution by increasing the ease of formation of adsorbed hydrogen species on the surface of iron.<sup>23</sup> While the importance of purity of the iron materials has been emphasized in previous research, such high values of charging efficiency of  $>90\%$  have not been reported in the literature.<sup>20</sup>

A further decrease in the rate of hydrogen evolution has been achieved by the addition of bismuth sulfide to the carbonyl iron

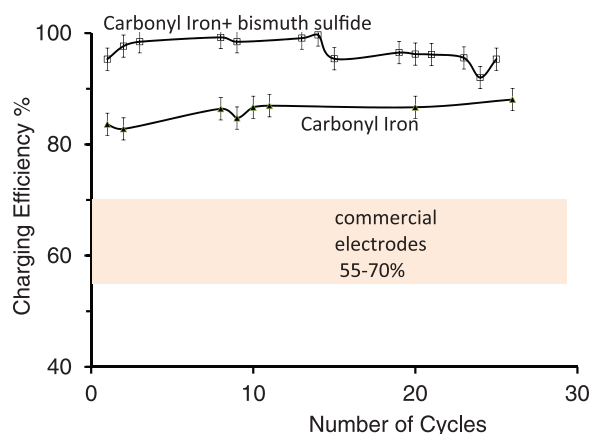


**Figure 5.** Charging efficiency as a function of cycling at  $C/2$  rate of charge and  $C/20$  rate of discharge. The band refers to the charging efficiency of state-of-art commercial electrodes from nickel-iron batteries (Sichuan Changhong Battery Co., Ltd., Sichuan, China) and data presented in References 14 and 15.

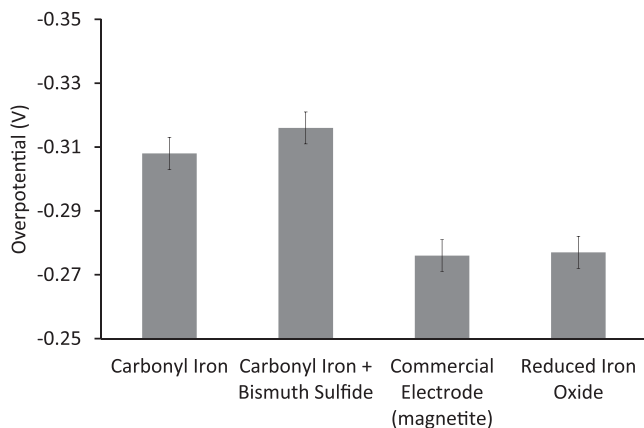


**Figure 6.** Hydrogen overpotential of various iron electrode materials during charging at  $C^*/10$  rate, where  $C^*$  is the theoretical capacity based on the mass of the electrode material.

material. Bismuth sulfide is an electrically conducting solid, insoluble in the potassium hydroxide electrolyte. During charging, the bismuth sulfide is transformed into elemental bismuth (Eq. 5).



The electrode potential for the reduction of bismuth sulfide to bismuth is more positive than that of the iron electrode reaction (Eq. 1) and thus the charging process conducted at  $-1$  V (vs NHE) facilitates the formation of elemental bismuth.<sup>24</sup> The presence of elemental bismuth in the charged electrodes was confirmed by X-ray powder diffraction (XRD) studies (Figure 7).

It is the presence of elemental bismuth that increases the overpotential for hydrogen evolution on carbonyl iron (Figure 6). The high hydrogen overpotential on bismuth is due to the unfavorable energetics for the electro-sorption of surface-bonded hydrogen intermediates.<sup>25</sup>

The kinetic parameters (exchange current and Tafel Slope) for the hydrogen evolution reaction on various iron electrodes were measured in the fully charged state where the only reaction resulting from the charging current is the hydrogen evolution reaction (Figure 8).

The exchange current, a measure of the kinetics of the hydrogen evolution process, is ten times lower for the bismuth-containing electrodes (Table I). Using the exchange current and Tafel slopes, we calculated (using Eq. 4) the current and electric charge diverted

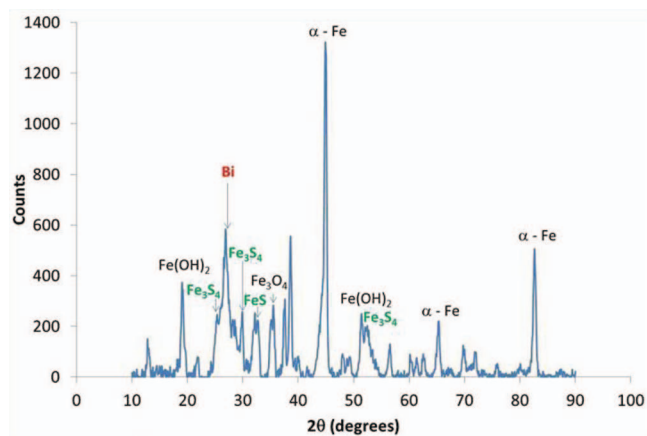


**Figure 7.** X-ray Diffractogram for a charged iron electrode prepared from carbonyl iron electrode and bismuth sulfide. Powder Diffraction Files: Fe (00-006-0696),  $\text{Fe}(\text{OH})_2$  (00-013-0089),  $\text{Fe}_3\text{O}_4$  (00-071-6766), Bi (00-044-1246),  $\text{Fe}_3\text{S}_4$  (01-089-1998),  $\text{FeS}$  (01-076-0964). Measurement was performed on a Rigaku Ultima IV (Cu  $K\alpha$ ) X-Ray Diffractometer.

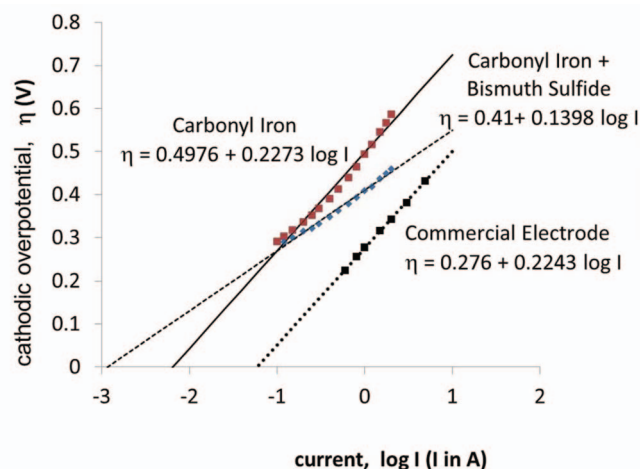


**Figure 8.** Cathodic Tafel polarization plots for fully-charged iron electrodes of various compositions. Parameters of the Tafel Equation are also shown.

to hydrogen evolution at any stage in the charging process. These calculations (Table I) confirm that the observed increased charging efficiency (Figures 4, 6) is due to the inhibition of the kinetics of hydrogen evolution by the in situ electrodeposition of elemental bismuth. The high overpotential for hydrogen evolution on bismuth is a property also exhibited by elemental forms of cadmium, lead, indium and mercury.<sup>17,18,25,26</sup> However, the latter elements are all highly toxic compared to bismuth and hence we considered them unsuitable for the large-scale energy storage applications.

The observation of bismuth as a separate phase even at a low fraction of 5% is consistent with the insolubility of bismuth in iron as predicted by the Hume-Rothery rules.<sup>27</sup> This insolubility combined with the low surface energies of bismuth makes the re-distribution of bismuth into the iron matrix highly unfavorable.<sup>28</sup> Consequently, the bismuth can be expected to remain on the surface of iron as nano-crystals or “ad-atoms” suppressing hydrogen evolution during charging. The bismuth present on the iron electrode does not undergo oxidation during the discharge process because the necessary electrode potential for electro-oxidation is not reached. In the event of over-discharge of the iron electrode, the bismuth will be oxidized to insoluble bismuth oxide. This bismuth oxide will be readily reduced to the elemental bismuth during the subsequent charge cycle.<sup>29</sup> These characteristics of the bismuth deposits are consistent with the stable charging efficiency values observed in repeated cycles of charge and discharge (Figure 5).

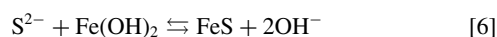
**Discharge Rate Capability.**— To meet the demands of large-scale energy storage, the batteries must be capable of being completely charged and discharged in one to two hours. The performance at different discharge rates is described by the term “rate-capability.” The higher the rate-capability the smaller the battery required for a particular amount of stored energy. For many of the redox-flow type batteries, charging and discharging at high rates results in significant loss of efficiency.<sup>30</sup> With the new carbonyl iron electrode containing bismuth sulfide, high discharge rate capability is achieved along with the improved charge efficiency. At a two-hour rate of discharge, with the addition of bismuth sulfide we observe a *twenty-fold increase in capacity* compared to the commercial electrode and a *fifty-fold increase* compared to the plain carbonyl iron electrode (Figure 9). We also note that the specific mass loading of the commercial electrodes is approximately 8 times higher than that of the carbonyl electrodes. This higher loading could also contribute to the lower rate capability of the commercial electrodes.

The specific discharge capacity of the electrode with bismuth sulfide even at a one-hour discharge rate corresponds to about 60% of the maximum discharge capacity of the electrode. The commercial

**Table I.** Kinetic parameters for hydrogen evolution on various iron electrodes. Charging efficiencies calculated based on Eq. 3. Exchange current was normalized for discharge capacity at twenty-hour rate.

| Electrode                       | Exchange current, (Amperes) | Discharge Capacity, (A hr) | Exchange current (A / A hr) | Tafel Slope, (Volt/decade of current) | Calculated Efficiency (%) | Measured Efficiency (%) |
|---------------------------------|-----------------------------|----------------------------|-----------------------------|---------------------------------------|---------------------------|-------------------------|
| Carbonyl Iron                   | $6.46 \times 10^{-3}$       | 0.36                       | $1.80 \times 10^{-2}$       | 0.227                                 | 71                        | 89                      |
| Carbonyl Iron + bismuth sulfide | $1.17 \times 10^{-3}$       | 0.64                       | $1.82 \times 10^{-3}$       | 0.140                                 | 84                        | 96                      |
| Commercial Electrode            | $5.86 \times 10^{-2}$       | 9.59                       | $6.11 \times 10^{-3}$       | 0.224                                 | 60                        | 55–70                   |

electrode yields almost no capacity at these high discharge rates. We attribute the excellent discharge rate capability of the electrodes formulated with bismuth sulfide to the in situ formation of iron sulfides. In the XRD measurements on cycled electrodes that incorporated bismuth sulfide, we were able to detect iron sulfide phases corresponding to FeS and Fe<sub>3</sub>S<sub>4</sub> (Figure 7). We may infer that sulfide ions (from reduction of bismuth sulfide (Eq. 5)) reacted with the iron (II) hydroxide to form iron (II) sulfide (Eq. 6).



The iron (II) sulfide can react with sulfide ions to form various mixed-valence iron sulfides that are electronically conductive like iron (II) sulfide. The in situ incorporation of such electronically conductive iron sulfides will counter the passivation caused by the discharge product, iron (II) hydroxide, an electronic insulator.<sup>17</sup>

Thus, the iron sulfide compounds maintain the electronic conductivity at the interface allowing the discharge reaction to be sustained at high rates. This is supported by previous work on the beneficial effect of sulfide additives.<sup>5,6,17,31,32</sup> The high charging-efficiency of 96% combined with a high level of utilization of 0.3 Ah g<sup>-1</sup> and fast discharge capability for the iron electrode achieved in this work allows us to develop a very inexpensive and efficient iron electrode.

An iron battery that stores 1 kWh of energy will require approximately 3 kg of iron powder at the specific capacity of 0.3 Ah/g. At the cost of \$1/kg (for high-purity iron in commercial quantities), the estimated cost of materials for the iron electrode is \$3 /kWh. Thus, the cost of the iron electrode can be as low as 3% of the cost target for large-scale energy storage. Such a low contribution to the cost from iron allows for generous cost allocations for other components such as the positive electrode, stacks and systems to meet the target of \$100/kWh for grid-scale electrical energy storage.

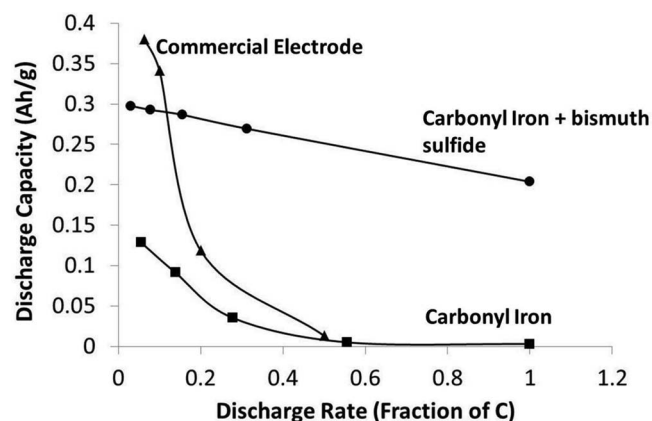


**Figure 9.** Discharge capacity of iron electrodes as function of the normalized discharge rate. Normalized discharge rate expressed as 1/n times the nominal capacity in Ampere-hours, where n is the number of hours of discharge (for e.g., 1/n = 0.5 corresponds to discharge in two hours of the entire capacity).

## Conclusions

In this work, we have shown a high-performance rechargeable iron electrode formulated with carbonyl iron and bismuth sulfide that is far superior in characteristics compared to a commercially available iron electrode. We achieve a *ten - fold reduction* in hydrogen evolution rate, a high *charging-efficiency of 96%*, a high *discharge capacity of 0.3 Ah g<sup>-1</sup>*, and also a *twenty-fold increase in capacity* for the two-hour discharge rate. The high level of purity of carbonyl iron combined with the in situ produced bismuth electro-deposits suppress the wasteful evolution of hydrogen, while the in situ formation of mixed-valent conductive iron sulfides facilitates high discharge rates. The efficiency and discharge performance were stable with repeated cycling. We have also shown that a viable “pressed-plate” type battery electrode can be inexpensively fabricated using this new formulation of active materials. These high-performance electrodes have broken the once-formidable barrier of low charging efficiencies and unneeded hydrogen evolution in iron-based aqueous alkaline batteries. Thus, both iron-air and nickel iron batteries can now become the basis for low-cost, durable, and efficient large-scale electrical energy storage systems.

## Acknowledgment

The research reported here was supported by the U.S. Department of Energy ARPA-E (GRIDS program, DE-AR0000136), the Loker Hydrocarbon Research Institute, and the University of Southern California. We thank Priyanka Narayan and Prof. Nagarajan Vaidehi for their very helpful comments.

## References

1. *Accommodating High Levels of Variable Generation*, North American Electric Reliability Corporation, April 2009.
2. Y. V. Makarov, B. Yang, J. G. DeSteele, S. Lu, C. H. Miller, P. Nyeng, J. Ma, D. J. Hamerstrom, and V. V. Viswanathan, *Wide-Area Energy Storage and Management System to Balance Intermittent Resources in the Bonneville Power Administration and California ISO Control Areas*, PNNL-17574 (June 2008).
3. B. Dunn, H. Kamat, and J.-M. Tarascon, *Science*, **334**, 928 (2011).
4. Z. Yang, J. Zhang, M. C. W. Kintner-Meyer, X. Lu, D. Choi, and J. P. Lemmon, *Chem. Rev.*, **111**, 3577, (2011).
5. K. Vijayamohan, A. K. Shukla, and S. Sathyanarayana, *J. Power Sources*, **32**, 329 (1990).
6. K. Vijayamohan, A. K. Shukla, and S. Sathyanarayana, *J. Electroanal. Chem.*, **295**, 59 (1990).
7. K. Vijayamohan, T. S. Balasubramanian, and A. K. Shukla, *J. Power Sources*, **34**, 269 (1991).
8. S. R. Narayanan, G. K. Surya Prakash, A. Manohar, B. Yang, S. Malkhandi, and A. Kindler, Materials challenges and technical approaches for realizing inexpensive and robust iron-air batteries for large scale energy storage, *Solid State Ionics*, In Press doi: 10.1016/j.ssi.2011.12.002.
9. S. R. Narayanan, G. K. Surya Prakash, and A. Kindler, Iron-air rechargeable battery, *US Patent 2010-366696P*, WO2012012731.
10. L. Ojefors and L. Carlsson, *J. Power Sources*, **2**, 287 (1977/78).
11. L. Ojefors, *Electrochim. Acta*, **21**, 263, (1976).
12. E. S. Buzzelli, C. T. Liu, and W. A. Bryant, Iron-Air batteries for electric vehicles, *Society of Automotive Engineers, Intersociety Energy Conversion Engineering Conference*, 13<sup>th</sup> Proceedings, SAE 789284, p. 745.
13. S. U. Falk and A. J. Salkind, *Alkaline Storage Batteries*, John Wiley (1969).
14. Beutliity Free, *Ni - Fe Batteries Product Data*.
15. Eagle Picher Industries, *Ni-Fe Batteries - Technical Data Sheet*.
16. B. J. Dougherty, F. L. Tanzella, and R. D. Weaver, Some Nickel-Iron, and Nickel-Metal Hydride, cell cycling results, *Proc. 10<sup>th</sup> Annual Battery Conference on Applications and Advances*, p. 199 (1995).

17. K. Vijayamohan, A. K. Shukla, and S. Sathyanarayana, *J. Electroanal. Chem.*, **289**, 55 (1990).
18. T. S. Balasubramanian, K. Vijayamohan, and A. K. Shukla, *J. Appl. Electrochem.*, **23**, 947 (1993).
19. K. Vijayamohan, A. K. Shukla, and S. Sathyanarayana, *Indian J. Tech.*, **24**, 430 (1986).
20. P. R. Vassie and A. C. C. Tseung, *Electrochim. Acta*, **21**, 299 (1976).
21. W. A. Bryant, *Electrochim. Acta*, **24**, 1057 (1974).
22. D. Linden, *Handbook of Batteries*, 2nd Edition, Mc-Graw Hill (1995).
23. R. Parsons, *Handbook of Electrochemical Constants*, Butterworths Scientific (1959).
24. G. Valyulene, A. Zhelene, V. Jasulaitene, and B. Shimkunaite, *Russian J. Appl. Chem.*, **80**, 1322 (2007).
25. J. O'M Bockris, in *Modern Aspects of Electrochemistry* (Ed. F. C. Tompkins), Academic Press (1954) p. 199.
26. M. K. Ravikumar, T. S. Balasubramanian, A. K. Shukla, and S. Venugopalan, *J. Appl. Electrochem.*, **26**, 1111 (1996).
27. W. Hume-Rothery, *The Structures of Alloys of Iron*, Pergamon Press, (1966) p. 132.
28. L. Vitos, A. V. Ruban, H. L. Skriver, and J. Kollár, *Surface Science*, **411**, 186 (1998).
29. G. H. Hwang, W. K. Han, S. J. Kim, S. J. Hong, J. S. Park, H. J. Park, and S. G. Kang, *J. Ceramic Proc. Res.*, **10**, 190 (2009).
30. D. Aaron, Z. Tang, A. B. Papandrew, and T. A. Zawodzinski, *J. Appl. Electrochem.*, **41**, 1175 (2011).
31. J. Cerny and K. Micka, *J. Power Sources*, **25**, 111 (1989).
32. K. Micka and Z. Zabransky, *J. Power Sources*, **19**, 315 (1987).